ATOMIC DATA AND NUCLEAR DATA TABLES **70,** 231–254 (1998)
ARTICLE NO. DT980793

IONIZATION STATE DISTRIBUTION AND RADIATIVE COOLING RATE FOR ARGON IN A LOW-DENSITY PLASMA*

K. B. FOURNIER, M. COHEN,† M. J. MAY,‡ and W. H. GOLDSTEIN

Lawrence Livermore National Laboratory
Livermore, California 94550

This paper presents the coronal ionization state distribution for argon. The calculations include *ab initio* rate coefficients for collisional excitation followed by autoionization (EA), and rates for direct ionization and dielectronic and radiative recombination. The EA rate coefficients have been fitted to analytical expressions, and the fitting coefficients are tabulated. The paper then presents the calculated radiative cooling coefficient for argon ions in a low-density plasma as a function of temperature. The channels for power loss from argon ions include collisional-radiative (CR) line emission, dielectronic and radiative recombination, and bremsstrahlung emission. The power emitted via CR line emission for each ion is tabulated on a grid of temperatures and densities. The total power loss coefficient is fitted to an analytical expression in powers of the temperature. © 1998 Academic Press

* The U.S. Government's right to retain a nonexclusive royalty-free license in and to the copyright covering this paper, for governmental purposes, is acknowledged.
† Permanent Address: Racah Institute of Physics, Hebrew University, Jerusalem, Israel.
‡ Plasma Spectroscopy Group, The Johns Hopkins University, Baltimore, MD 21218.

0092-640X/98 $25.00

CONTENTS

INTRODUCTION

Radiation from intrinsic impurities in a magnetically confined fusion plasma removes energy from the fusion reaction, is detrimental to the global energy confinement, and dilutes the reaction fuel [1, 2]. On the other hand, radiation in the outermost region of the plasma from deliberately introduced impurities is seen as a possible mechanism for controlling the heatload deposited onto the plasma facing components of a fusion reactor [3, 4]. Inert gases (Ne, Ar, and Kr) are seen as potentially useful in this regard [5, 6]. Thus, the radiative patterns of impurity elements in a fusion plasma must be understood across the range of temperatures achieved in present-day experiments. This paper makes available calculations of the coronal ionization state distribution and the total radiative cooling coefficient for argon from 2 eV to 20 keV. The present work applies *ab initio*, relativistic calculations of multistep ionization rates [7] to computing the argon charge state distribution (CSD). Then, detailed collisional-radiative (CR) models are used to calculate the radiative cooling coefficient for argon in a low density plasma. The excitation autoionization (EA) rates of the present work and the total cooling coefficient are fitted to analytical expressions for ease of use in plasma modeling codes.

Charge State Distribution

An integral part of the radiative cooling coefficient calculation for argon described below is the (coronal) charge state distribution. The relative populations of two adjacent ionization states of element Z are given (in the coronal limit) by

$$\frac{n_Z^{q+1}}{n_Z^q} = \frac{S^q(T_e)}{\alpha^{q+1}(T_e)}, \tag{1}$$

where $S^q(T_e)$ is the total rate of ionization out of the ground level of ion $q+$, and $\alpha^{q+1}(T_e)$ is the total rate of recombination out of the ground level of ion $(q+1)+$. The total rate of ionization includes the contribution from direct electron impact ionization (DI) and collisional excitation followed by autoionization. The total rate of recombination includes contributions from radiative (RR) and dielectronic recombination (DR). By requiring that

$$\sum_q n_z^q = 1$$

for each temperature, where the sum is over the population in the ground level of all ions, the fractional abundance of each ionization stage is found. The CSD calculated for argon is shown in Fig. 1. The fractional abundance of each ion is tabulated in Table I.

Two channels for recombination have been considered in Eq. (1): direct capture of a free electron followed by the emission of a photon (RR) and the capture of a free electron

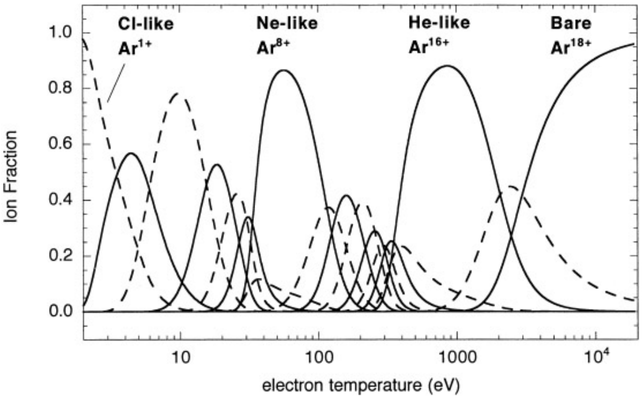

FIG. 1. Coronal charge state distribution for argon in the range from T_e = 2 eV to 20 keV.

into a doubly excited autoionizing level followed by radiative stabilization (DR). The rate coefficients for the RR process have been found using detailed balance of photoionization cross sections calculated with the Hartree–Slater code of Scofield [8]. The rates of DR have been taken from Mazzotta et al. [9]. The contribution of RR to the total recombination rate is less than that of DR for nearly every argon ion. Two channels of ionization have been considered: direct ionization by electron collision and collisional excitation to an energy level in the continuum followed by autoionization. Details about the EA data are given below. The contribution of DI from both valence and inner-shell orbitals to the total ionization rate has been evaluated using the Lotz formula [10, 11] and a relativistic calculation of subshell binding energies [12]. For the direct processes above, DI and RR, the rate coefficients used in the present work are within a few percent of those computed by other methods and available in previous tabulations [13]. The rate coefficients for RR, DI, and DR from the ground level of each argon ion (including the fully stripped and neutral charge states) are shown in Graphs 1–3, 4–7, and 8–11, respectively, after Tables I to IV.

Excitation Autoionization

EA contributes substantially to the total rate of ionization in the ions near the closed-shell Ne-like Ar^{8+}, that is, in Ar^{5+}, Ar^{6+}, and Ar^{7+}. For EA, we have used the data in Ref. [7] in the calculation of the argon CSD. In order to have a better resolution of the EA rate coefficients, we have also computed the EA rate coefficients for Ar^{15+} to Ar^{2+} at temperatures intermediate to those reported in Ref. [7]. Further, for Ar^{6+} to Ar^{9+} we have extended the calculations to lower temperatures ($T_e \gtrsim 5$ eV). These data have been fitted to the formula

$$S_{fit}^{EA}(T_e) = 1.0 \times 10^{-Y} \sum_{i=1}^{3} \frac{c_i}{T_e^{1/2}} \exp(-d_i/T_e), \qquad (2)$$

where T_e is in eV, and the EA rate coefficients are in units of $\mathrm{cm}^3\ \mathrm{s}^{-1}$. The resulting fitting coefficients are given in Table II (for Ar^{15+} to Ar^{2+}). The EA fitting formula reproduces the calculated rates [7] to better than 5% everywhere except at the low end of the temperature range indicated for each ion, where the formula may underestimate the *ab initio* EA rate coefficients by up to a factor of $\approx$4 in some cases. The larger deviations typically occur for the more highly ionized stages and generally at temperatures well below the region of maximum abundance for the ion in question. Where the large deviations occur closer to maximum abundance (as in Ar^{14+} and Ar^{15+}), they are inconsequential for the CSD since DI is by far the dominant process in those instances. The ground level EA rate coefficients computed from Eq. (2) for each ion considered are shown in Graphs 12–14, after Tables I to IV.

Radiative Cooling Coefficient

The method used to calculate the argon radiative cooling coefficient is described in our previous work [14, 15] for the molybdenum cooling coefficient. Power losses for argon from CR line emission and line emission from DR and continuum radiation from RR and bremsstrahlung are considered. We now briefly remind the reader of some of the quantities computed.

The power loss coefficient for CR line emission from an ion (with charge $q+$) at a fixed temperature is given by

$$L_q^{CR}(T_e) = \sum_{jf} \frac{hc}{\lambda_{jf}} \times J_{jf}(T_e), \qquad (3)$$

where $J_{jf}(T_e)$ (in units of photons cm^3/s) is found from the collisional-radiative model, λ_{jf} is the transition wavelength, and the sum is taken over all possible radiative transitions (including "forbidden" decays). Our collisional-radiative models include all possible promotions of valence and inner-shell bound electrons to all available vacancies with principal quantum number $n \leq 5$. Even at high temperatures, where higher n levels can be populated, this set of models accounts for $\gtrsim 97\%$ of the power emitted by each ion. The amount of power radiated per unit volume by collisional-radiative line emission from an impurity atom (with atomic number Z) is given by

$$P_Z^{CR}(T_e) = n_e \sum_q n_q L_q^{CR}(T_e), \qquad (4)$$

where n_q is the number density of an impurity ion of charge $q+$, n_e is the electron density, and the sum is taken over all charge states of the atom. The sum in Eq. (4) can be expressed as

$$P_Z^{CR}(T_e) = n_e n_Z \sum_q f_q^{CE}(T_e)\, L_q^{CR}(T_e), \tag{5}$$

where n_Z is the total number density of atom Z and $f_q^{CE}(T_e)$, the coronal equilibrium fractional abundance of ion $q+$, is given in Table I. Thus, the power lost per unit volume can be written as

$$P_Z^{CR}(T_e) = n_e n_Z L_Z^{CR}(T_e), \tag{6}$$

where $L_Z^{CR}(T_e)$ is the *radiative cooling coefficient* for line emission from element Z. For low-density, collisionally ionized plasmas (such as those in a tokamak), an ion will have its maximal abundance (in equilibrium) at a temperature between 20 and 50% of its ionization energy. Three temperature grids, each with six points, have been selected for calculation of the CR models: 5, 10, 15, . . . , 30%, and 10, 20, 30, . . . , 60%, and 20, 40, 60, . . . , 120% of the ionization potential of each ion. An examination of the temperatures for which each ionization state has an abundance >1% has determined which grid is appropriate for computing the power loss coefficient in Eq. (3). The CR line power loss rate for *each* argon ion, $n_e L_q^{CR}(T_e)$ (in erg s^{-1}), is tabulated in Table III for six temperatures and densities. The power scales linearly with the electron density (for most ions at most temperatures), indicating that most of the power is lost only via transitions fed from the ground level and that our assumption of coronal equilibrium is appropriate.

When the temperature considered for computing the radiative cooling coefficient in Eq. (5) is between the temperatures explicitly computed for the CR models, the emissivity of that ion is found by linear interpolation,

$$L_q^{CR}(T_e) = L_q^{CR}(T_{\text{lower}})\left(1 - \frac{T_e - T_{\text{lower}}}{T_{\text{upper}} - T_{\text{lower}}}\right) + L_q^{CR}(T_{\text{upper}})\left(\frac{T_e - T_{\text{lower}}}{T_{\text{upper}} - T_{\text{lower}}}\right), \tag{7}$$

where T_{lower} and T_{upper} are the closest temperatures in the CR model grid to the temperature under consideration. When the temperature in Eq. (5) is lower than any of the calculated temperatures for an ion, the emissivity of that ion is found by scaling

$$L_q^{CR}(T_e) = L_q^{CR}(T_{\text{lowest}})\left(\frac{T_e}{T_{\text{lowest}}}\right), \tag{8}$$

which ensures that $L_q^{CR}(T_e) \to 0$ as $T_e \to 0$. When the temperature under consideration is higher than any of the temperatures in the Eq. (3) calculation, we find the emissivity of that ion at that temperature by extrapolating upward

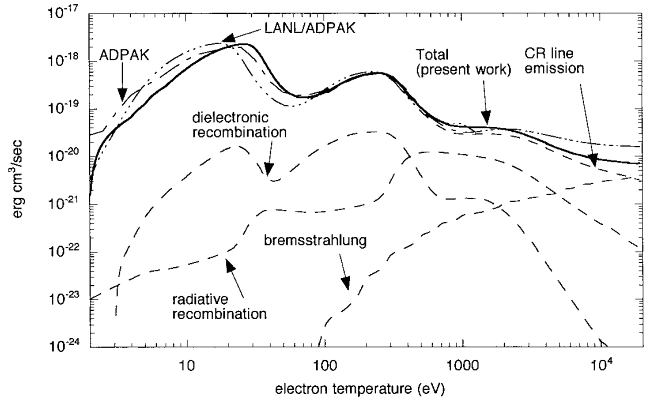

FIG. 2. Calculated total radiative loss coefficient (solid line) for argon. Also shown are the radiative loss coefficients for CR line emission (dashes, cf. Eq. (3)), DR and RR emission and bremsstrahlung (all dashes). The total radiative loss coefficient for argon from the original ADPAK [16] code (dash–dot) and a modified ADPAK [18] (dash–dot–dot–dot) are also shown.

$$L_q^{CR}(T_e) = L_q^{CR}(T_{\text{highest}-1})\left(1 - \frac{T_e - T_{\text{highest}-1}}{T_{\text{highest}} - T_{\text{highest}-1}}\right) + L_q^{CR}(T_{\text{highest}})\left(\frac{T_e - T_{\text{highest}-1}}{T_{\text{highest}} - T_{\text{highest}-1}}\right), \tag{9}$$

where T_{highest} and $T_{\text{highest}-1}$ are the two highest temperatures in the CR model grid for an ion. Since our grids are optimized to cover temperatures where an ion has a >1% fractional abundance, the extrapolations beyond the grid introduce a minimal amount of uncertainty in our calculation.

Figure 2 shows the *total* radiative loss coefficient (solid line) for argon. For temperatures from 2 eV to 20 keV, the CR line emission (dashes) dominates the total radiative loss coefficient; the only place the CR line emission coefficient differs appreciably from the total radiative cooling coefficient is above 10 keV, where the argon ions are almost fully stripped. The radiative cooling coefficients for DR and RR emission and bremsstrahlung (all dashes) are also shown in Fig. 2. The radiative power loss coefficient from DR line emission is approximated using the formula in Ref. [16], computed level energies [12], and the DR rate coefficients in Ref. [9]. The volumetric power loss from RR continuum emission is also approximated using the formula in Ref. [16], the average charge on an argon ion at electron temperature T_e as shown in Fig. 1, and the radiative recombination rate coefficients described above. Bremsstrahlung continuum emission power losses have been computed using the formula of Ref. [17] and the average charge on an argon ion as shown in Fig. 1. For comparison, two calculations of the total power loss coefficient by other authors are also shown. The total radiative loss coefficient for argon (including radiative channels fed by various recombination processes) from the ADPAK package [16] is given by the dashes; a recent update of the ADPAK radiative loss coefficient for argon by Clark et al. [18], which employs detailed collisional-radiative models below 2000 eV, is given by the dash–dot–dot–dot trace. The total radiative cooling coefficient (the sum of all channels shown in Fig. 2) in erg $\mathrm{cm}^3\ \mathrm{s}^{-1}$ has been fitted (in different temperature ranges) to an expression of the form

$$L_Z^{\mathrm{total}}(T_e) = \sum_{i=0}^{5} M_i T_e^i, \tag{10}$$

where T_e is in keV, and the values of M_i, the coefficients of the fit, are listed in Table IV.

Acknowledgments

K.B.F. would thanks Dr. D. Post of the ITER U.S. Home Team for making available the LANL/ADPAK argon models and Dr. G. Mazzitelli at the ENEA Frascati research facility for making available his tabulations of rate coefficients before their publication. This work was performed under the auspices of the U.S. Department of Energy at the Lawrence Livermore National Laboratory under Contract W-7405-ENG-48.

References

1. C. DeMichelis and M. Mattioli, Rep. Prog. Phys. **47,** 1233 (1984)
2. D. E. Post, J. Abdallah, R. Clark, and N. Putvinskaya, Phys. Plasmas **2,** 2328 (1995)
3. Y. Shimomura, Nucl. Fusion **17,** 626 (1977)
4. D. E. Post, J. Nucl. Mater. **222,** 143 (1995)
5. J. Cummings et al., J. Nucl. Mater. **176–177,** 916 (1990)
6. J. Mandrekas, W. M. Stacey, and F. Kelly, Nucl. Fusion **36,** 917 (1996)
7. M. Cohen, K. B. Fournier, and W. H. Goldstein, Phys. Rev. A **57,** 2651 (1998)
8. E. B. Saloman, J. H. Hubble, and J. H. Scofield, Atomic Data and Nuclear Data Tables **38,** 1 (1988)
9. P. Mazzotta, G. Mazzitelli, S. Colafrancesco, and N. Vittorio, Astron. Astrophys. Suppl. Ser., to appear; preprint available at xxx.lanl.gov/format/astro-ph/9806391.
10. W. Lotz, Z. Phys. **216,** 241 (1968)
11. W. Lotz, Z. Phys. **232,** 101 (1970)
12. M. Klapisch, J. Schwob, B. Fraenkel, and J. Oreg, J. Opt. Soc. Am. **67,** 148 (1977)
13. M. Arnaud and R. Rothenflug, Astron. Astrophys. Suppl. Series **60,** 425 (1985)
14. K. B. Fournier et al., Nucl. Fusion **37,** 825 (1997)
15. K. B. Fournier et al., Nucl. Fusion **38,** 639 (1998)
16. D. E. Post et al., Atomic Data and Nuclear Data Tables **20,** 397 (1977)
17. K. Kadota, M. Otsuka, and J. Fujita, Nucl. Fusion **20,** 209 (1980)
18. R. Clark, J. Abdallah, and D. E. Post, J. Nucl. Mater. **220–222,** 1028 (1995).

EXPLANATION OF TABLES

TABLE I. Argon Charge State Fractional Populations

T_e	Electron temperature in eV.

Fractional population in each charge state at a given temperature is listed below each ion.

TABLE II. Fitting Coefficients for Argon Excitation Autoionization (EA) Rates

Ion	The argon ion under consideration; the temperature range over which the EA coefficients have been fitted is indicated above each ion.
Level	The energy level in the ground configuration of the ion under consideration; “gl” is the true ground level, g2 . . . are numbered in order of increasing energy.
k	The number of electrons in the expression for the EA channel above each block of coefficients.
Y	The exponent required for the fit given by Eq. (2).
c_i, d_i	The coefficients of the fit given by Eq. (2).
R	The multiple-correlation coefficient for the fit given by Eq. (2).

TABLE III. Radiative Cooling Rate for Argon Ions

Radiative Cooling Rate	The collisional radiative cooling rate $n_e L^{CR}(T_e)$ in erg s^{-1} for the ion listed at the head of the data block; numbers in square brackets represent powers of 10; i.e., $X[-Y] = X \times 10^{-Y}$.
n_e	The electron density in cm^{-3} at which the radiative cooling rate is computed.
T_e	The electron temperature in eV at which the radiative cooling rate coefficient is computed.

TABLE IV. Fitting Coefficients for Argon Cooling Coefficient

T_e	The electron temperature range in keV.
M_j	The coefficients of the fit given by Eq. (10); numbers in square brackets represent powers of 10; i.e., $X[-Y] = X \times 10^{-Y}$.

EXPLANATION OF GRAPHS

GRAPHS. Ground Level Rate Coefficients

Ordinate	Ground level rate coefficient in $cm^3\ s^{-1}$.
	RR: Radiative recombination, Graphs 1–3.
	DI: Direct ionization, Graphs 4–7.
	DR: Dielectronic recombination, Graphs 8–11.
	EA: Excitation autoionization, Graphs 12–14.
Abscissa	Electron temperature in eV.

TABLE I. Argon Charge State Fractional Populations

See page 236 for Explanation of Tables

T_e	Ar^{1+}	Ar^{2+}	Ar^{3+}	Ar^{4+}	Ar^{5+}	Ar^{6+}	Ar^{7+}	Ar^{8+}	Ar^{9+}	Ar^{10+}
1.5	1.000	–	–	–	–	–	–	–	–	–
1.7	0.999	0.001	–	–	–	–	–	–	–	–
2.0	0.973	0.027	–	–	–	–	–	–	–	–
2.5	0.801	0.199	–	–	–	–	–	–	–	–
3.0	0.629	0.368	0.003	–	–	–	–	–	–	–
4.0	0.385	0.551	0.064	–	–	–	–	–	–	–
4.5	0.302	0.568	0.130	–	–	–	–	–	–	–
5.0	0.213	0.543	0.244	–	–	–	–	–	–	–
6.1	0.110	0.431	0.458	0.002	–	–	–	–	–	–
7.5	0.043	0.272	0.671	0.013	–	–	–	–	–	–
8.0	0.033	0.232	0.715	0.021	–	–	–	–	–	–
8.9	0.019	0.168	0.768	0.046	–	–	–	–	–	–
9.8	0.012	0.126	0.782	0.080	0.001	–	–	–	–	–
10.5	0.008	0.100	0.775	0.116	0.002	–	–	–	–	–
11.4	0.005	0.074	0.743	0.175	0.004	–	–	–	–	–
12.2	0.003	0.057	0.703	0.228	0.008	–	–	–	–	–
13.1	0.002	0.041	0.637	0.301	0.018	–	–	–	–	–
13.9	0.001	0.032	0.576	0.360	0.030	0.001	–	–	–	–
15.4	0.001	0.019	0.463	0.450	0.065	0.002	–	–	–	–
16.5	–	0.013	0.382	0.497	0.103	0.005	–	–	–	–
17.5	–	0.010	0.321	0.519	0.141	0.009	–	–	–	–
17.7	–	0.009	0.307	0.522	0.151	0.010	–	–	–	–
18.9	–	0.006	0.240	0.526	0.207	0.021	–	–	–	–
20.3	–	0.004	0.174	0.502	0.277	0.043	0.001	–	–	–
21.4	–	0.002	0.136	0.471	0.323	0.065	0.002	–	–	–
21.9	–	0.002	0.121	0.453	0.343	0.078	0.002	0.001	–	–
23.5	–	0.001	0.081	0.388	0.394	0.127	0.006	0.002	–	–
24.3	–	0.001	0.066	0.352	0.411	0.157	0.009	0.004	–	–
25.4	–	0.001	0.049	0.304	0.422	0.199	0.015	0.010	–	–
28.3	–	–	0.022	0.187	0.392	0.301	0.042	0.056	–	–
30.1	–	–	0.012	0.127	0.334	0.336	0.066	0.124	–	–
32.3	–	–	0.006	0.073	0.246	0.330	0.094	0.252	–	–
34.6	–	–	0.002	0.038	0.159	0.280	0.112	0.408	–	–
36.9	–	–	0.001	0.018	0.095	0.213	0.117	0.555	0.001	–
39.7	–	–	–	0.008	0.050	0.147	0.112	0.681	0.002	–
41.5	–	–	–	0.004	0.034	0.115	0.107	0.737	0.003	–
44.8	–	–	–	0.002	0.017	0.075	0.097	0.803	0.006	–
47.9	–	–	–	0.001	0.009	0.053	0.089	0.837	0.010	–
50.3	–	–	–	0.001	0.006	0.041	0.084	0.853	0.015	–
52.3	–	–	–	–	0.005	0.034	0.080	0.860	0.020	–
55.3	–	–	–	–	0.003	0.026	0.076	0.866	0.029	–
58.3	–	–	–	–	0.002	0.021	0.072	0.865	0.040	0.001
63.6	–	–	–	–	0.001	0.014	0.065	0.852	0.066	0.002
66.4	–	–	–	–	0.001	0.011	0.062	0.841	0.082	0.003
68.3	–	–	–	–	0.001	0.010	0.060	0.832	0.094	0.004
72.2	–	–	–	–	–	0.008	0.055	0.809	0.121	0.007
75.1	–	–	–	–	–	0.007	0.052	0.788	0.143	0.010
78.2	–	–	–	–	–	0.005	0.049	0.764	0.166	0.015
80.7	–	–	–	–	–	0.005	0.046	0.742	0.187	0.020
85.0	–	–	–	–	–	0.004	0.042	0.703	0.220	0.031

TABLE I. Argon Charge State Fractional Populations

See page 236 for Explanation of Tables

T_e	Ar^{7+}	Ar^{8+}	Ar^{9+}	Ar^{10+}	Ar^{11+}	Ar^{12+}	Ar^{13+}	Ar^{14+}	Ar^{15+}	Ar^{16+}
85.5	0.041	0.697	0.225	0.032	0.001	–	–	–	–	–
89.9	0.037	0.653	0.258	0.048	0.002	–	–	–	–	–
93.8	0.033	0.610	0.287	0.065	0.003	–	–	–	–	–
96.7	0.031	0.578	0.305	0.080	0.004	–	–	–	–	–
100.2	0.028	0.538	0.326	0.101	0.006	–	–	–	–	–
103.7	0.025	0.498	0.343	0.124	0.009	–	–	–	–	–
106.1	0.023	0.470	0.353	0.141	0.012	–	–	–	–	–
109.2	0.020	0.436	0.362	0.164	0.016	–	–	–	–	–
112.3	0.018	0.402	0.369	0.187	0.021	0.001	–	–	–	–
120.7	0.013	0.318	0.373	0.253	0.041	0.002	–	–	–	–
125.3	0.011	0.275	0.367	0.287	0.056	0.003	–	–	–	–
128.7	0.010	0.247	0.359	0.311	0.069	0.004	–	–	–	–
132.8	0.008	0.216	0.346	0.337	0.087	0.006	–	–	–	–
137.0	0.007	0.187	0.331	0.361	0.107	0.008	–	–	–	–
140.5	0.006	0.165	0.316	0.377	0.125	0.011	0.001	–	–	–
144.9	0.005	0.141	0.296	0.394	0.148	0.015	0.001	–	–	–
150.7	0.004	0.113	0.268	0.409	0.182	0.022	0.002	–	–	–
156.0	0.003	0.092	0.243	0.416	0.212	0.031	0.003	–	–	–
159.9	0.002	0.080	0.225	0.417	0.234	0.038	0.004	–	–	–
163.0	0.002	0.070	0.211	0.415	0.252	0.045	0.005	–	–	–
166.9	0.002	0.060	0.193	0.411	0.273	0.054	0.006	–	–	–
167.7	0.002	0.058	0.190	0.410	0.277	0.056	0.006	–	–	–
170.1	0.001	0.053	0.179	0.406	0.290	0.062	0.008	0.001	–	–
180.7	0.001	0.035	0.138	0.378	0.337	0.094	0.015	0.001	–	–
185.8	0.001	0.028	0.121	0.361	0.356	0.111	0.020	0.002	–	–
192.6	–	0.021	0.101	0.334	0.374	0.135	0.029	0.004	–	–
195.2	–	0.019	0.094	0.324	0.380	0.144	0.033	0.005	–	–
199.6	–	0.016	0.083	0.306	0.387	0.160	0.040	0.006	–	–
201.4	–	0.015	0.079	0.298	0.389	0.167	0.043	0.007	0.001	–
205.9	–	0.012	0.070	0.279	0.393	0.183	0.052	0.009	0.001	–
210.5	–	0.010	0.061	0.260	0.393	0.199	0.062	0.013	0.001	–
215.1	–	0.008	0.053	0.241	0.391	0.215	0.072	0.016	0.002	–
219.7	–	0.007	0.046	0.223	0.387	0.229	0.084	0.021	0.003	–
220.7	–	0.007	0.045	0.219	0.386	0.232	0.086	0.022	0.003	–
222.6	–	0.006	0.042	0.211	0.383	0.238	0.091	0.024	0.003	0.001
226.4	–	0.005	0.038	0.197	0.376	0.248	0.102	0.029	0.004	0.001
229.3	–	0.005	0.034	0.186	0.370	0.255	0.110	0.033	0.005	0.001
235.1	–	0.004	0.029	0.166	0.356	0.268	0.126	0.042	0.007	0.002
241.1	–	0.003	0.024	0.146	0.339	0.278	0.144	0.054	0.010	0.003
246.1	–	0.002	0.020	0.131	0.323	0.284	0.158	0.064	0.014	0.004
249.1	–	0.002	0.018	0.122	0.313	0.286	0.166	0.072	0.016	0.005
252.2	–	0.002	0.016	0.114	0.302	0.288	0.175	0.079	0.018	0.006
255.3	–	0.002	0.015	0.106	0.291	0.289	0.183	0.087	0.021	0.007
257.4	–	0.001	0.014	0.100	0.284	0.289	0.188	0.092	0.024	0.008
258.4	–	0.001	0.013	0.098	0.280	0.289	0.190	0.095	0.025	0.009
260.5	–	0.001	0.012	0.093	0.272	0.288	0.195	0.101	0.027	0.010
262.6	–	0.001	0.011	0.088	0.264	0.287	0.200	0.107	0.030	0.011
263.7	–	0.001	0.011	0.086	0.260	0.286	0.203	0.110	0.031	0.012
265.8	–	0.001	0.010	0.081	0.252	0.285	0.207	0.116	0.034	0.013
269.0	–	0.001	0.009	0.075	0.240	0.282	0.213	0.125	0.039	0.016

TABLE I. Argon Charge State Fractional Populations
See page 236 for Explanation of Tables

T_e	Ar^{8+}	Ar^{9+}	Ar^{10+}	Ar^{11+}	Ar^{12+}	Ar^{13+}	Ar^{14+}	Ar^{15+}	Ar^{16+}	Ar^{17+}	Ar^{18+}
270.1	0.001	0.009	0.073	0.236	0.281	0.215	0.128	0.040	0.017	–	–
275.5	0.001	0.007	0.063	0.216	0.273	0.224	0.144	0.049	0.023	–	–
281.0	–	0.006	0.054	0.196	0.264	0.230	0.160	0.059	0.030	–	–
285.4	–	0.005	0.048	0.181	0.255	0.234	0.173	0.067	0.036	–	–
291.0	–	0.004	0.040	0.162	0.242	0.237	0.189	0.079	0.046	–	–
300.1	–	0.003	0.031	0.134	0.219	0.236	0.211	0.100	0.067	–	–
310.6	–	0.002	0.022	0.105	0.191	0.229	0.232	0.124	0.096	–	–
320.2	–	0.001	0.016	0.083	0.165	0.217	0.244	0.146	0.127	–	–
331.1	–	0.001	0.011	0.063	0.136	0.198	0.252	0.170	0.169	–	–
342.4	–	0.001	0.007	0.046	0.110	0.177	0.252	0.191	0.216	–	–
350.0	–	–	0.006	0.037	0.095	0.162	0.248	0.203	0.249	–	–
360.3	–	–	0.004	0.028	0.076	0.142	0.240	0.216	0.294	–	–
374.9	–	–	0.002	0.018	0.056	0.116	0.222	0.228	0.358	–	–
401.0	–	–	0.001	0.009	0.031	0.077	0.184	0.235	0.463	–	–
415.3	–	–	0.001	0.006	0.023	0.062	0.164	0.232	0.513	–	–
429.9	–	–	–	0.004	0.016	0.049	0.144	0.227	0.559	–	–
446.4	–	–	–	0.002	0.011	0.038	0.125	0.219	0.604	–	–
460.2	–	–	–	0.002	0.009	0.031	0.110	0.211	0.637	–	–
476.0	–	–	–	0.001	0.006	0.024	0.096	0.202	0.670	–	–
500.3	–	–	–	0.001	0.004	0.017	0.078	0.188	0.712	–	–
513.7	–	–	–	–	0.003	0.014	0.069	0.180	0.732	0.001	–
539.5	–	–	–	–	0.002	0.010	0.056	0.167	0.764	0.001	–
579.0	–	–	–	–	0.001	0.006	0.042	0.149	0.800	0.002	–
624.7	–	–	–	–	0.001	0.004	0.031	0.132	0.830	0.003	–
675.2	–	–	–	–	–	0.002	0.022	0.117	0.853	0.005	–
751.3	–	–	–	–	–	0.001	0.015	0.100	0.873	0.011	–
800.2	–	–	–	–	–	0.001	0.012	0.092	0.879	0.016	–
872.0	–	–	–	–	–	0.001	0.009	0.082	0.881	0.027	–
999.9	–	–	–	–	–	–	0.006	0.069	0.869	0.056	0.001
1499.6	–	–	–	–	–	–	0.001	0.036	0.689	0.247	0.027
1999.1	–	–	–	–	–	–	–	0.017	0.446	0.408	0.128
2004.6	–	–	–	–	–	–	–	0.017	0.443	0.409	0.130
2504.5	–	–	–	–	–	–	–	0.008	0.262	0.448	0.282
3003.9	–	–	–	–	–	–	–	0.004	0.155	0.414	0.427
4000.7	–	–	–	–	–	–	–	0.001	0.062	0.310	0.627
5003.6	–	–	–	–	–	–	–	–	0.030	0.232	0.738
6001.6	–	–	–	–	–	–	–	–	0.017	0.180	0.803
7014.1	–	–	–	–	–	–	–	–	0.010	0.145	0.845
8003.8	–	–	–	–	–	–	–	–	0.007	0.121	0.872
9015.2	–	–	–	–	–	–	–	–	0.005	0.102	0.893
10019.0	–	–	–	–	–	–	–	–	0.003	0.089	0.908
11016.0	–	–	–	–	–	–	–	–	0.003	0.078	0.919
12014.0	–	–	–	–	–	–	–	–	0.002	0.070	0.928
13033.0	–	–	–	–	–	–	–	–	0.002	0.063	0.935
14019.0	–	–	–	–	–	–	–	–	0.001	0.057	0.941
15043.0	–	–	–	–	–	–	–	–	0.001	0.053	0.946
19000.0	–	–	–	–	–	–	–	–	0.001	0.039	0.960

TABLE II. Fitting Coefficients for Argon Excitation Autoionization (EA) Rates

See page 236 for Explanation of Tables

Ion	Level	k	Y	c_1	d_1	c_2	d_2	c_3	d_3	R
				$1s^2 2l^k \rightarrow 1s2l^k n'l' + 1s^2 2l^{k-1} n'l'$						
				temperature range of fits 200 to 4000eV						
Ar^{15+}	g1	1	11	43.762	3516.8					0.9997
				temperature range of fits 200 to 3000eV						
Ar^{14+}	g1	2	11	3.6075	1703.7	102.51	3713.3			0.99996
				temperature range of fits 110 to 3000eV						
Ar^{13+}	g1	3	11	18.277	834.57	88.904	3705.9			0.99996
	g2		11	20.754	834.47	86.491	3684.3			0.99996
				temperature range of fits 50 to 3000eV						
Ar^{12+}	g1	4	12	−3.5579	467.60	423.03	724.87	242.23	3035.1	0.99994
	g2		12	31.608	506.16	430.75	775.35	287.32	3535.4	0.99993
	g3		12	492.240	737.77	332.52	3339.10	−1.4204	4380.1	0.99996
	g4		12	685.100	713.49	−5.1491	873.32	441.42	3173.9	0.99997
	g5		12	167.400	520.65	795.40	787.64	584.00	3606.9	0.99998
Ar^{11+}	g1	5	11	68.325	677.29	49.354	2994.8			0.99997
	g2		11	102.420	653.12	72.150	3022.2			0.99997
	g3		11	104.110	653.00	73.108	3020.2			0.99997
	g4		11	169.850	640.77	116.110	2943.3			0.99997
	g5		11	170.970	641.17	118.490	2947.2			0.99997
Ar^{10+}	g1	6	11	193.29	591.49	144.53	2705.5			0.99996
	g2		11	200.44	589.97	150.34	2706.2			0.99996
	g3		11	203.10	589.45	152.37	2701.3			0.99996
	g4		11	223.02	579.65	149.23	2646.4			0.99997
	g5		11	300.73	573.94	220.79	2662.9			0.99996
				temperature range of fits 40 to 3000eV						
Ar^{9+}	g1	7	11	314.37	533.08	234.46	2513.6			0.99995
	g2		11	327.04	531.27	242.40	2507.6			0.99995
				temperature range of fits 20 to 2000eV						
Ar^{8+}	g1	8	11	394.33	468.94	264.78	1921.6			0.99999

TABLE II. Fitting Coefficients for Argon Excitation Autoionization (EA) Rates

See page 236 for Explanation of Tables

Ion	Level	k	Y	c_1	d_1	c_2	d_2	c_3	d_3	R
				$1s^22l^83l^k \rightarrow 1s^22l^73l^kn'l' + 1s^22l^83l^{k-1}n'l'$						
				temperature range of fits 15 to 2000eV						
Ar^{7+}	g1	1	10	705.37	335.34	727.95	1596.6			0.99992
				temperature range of fits 10 to 2000eV						
Ar^{6+}	g1	2	10	692.43	282.30	773.30	1416.4			0.99983
Ar^{5+}	g1	3	10	186.62	111.13	679.53	374.13	706.29	1828.8	0.99998
	g2		10	185.97	112.34	682.46	373.95	706.77	1823.8	0.99998
				temperature range of fits 25 to 2000eV						
Ar^{4+}	g1	4	9	23.583	85.614	62.625	353.54	62.606	1778.4	0.99977
	g2		9	23.624	85.627	61.797	352.27	61.035	1777.3	0.99977
	g3		9	23.485	85.755	61.785	351.64	61.362	1772.5	0.99977
	g4		9	26.592	82.937	63.106	352.45	62.285	1789.3	0.99976
	g5		9	35.260	79.540	69.021	352.50	68.107	1796.4	0.99973
				temperature range of fits 10 to 400eV						
Ar^{3+}	g1	5	10	299.49	65.835	331.74	298.88			0.99992
	g2		10	432.51	61.370	328.28	287.91			0.99995
	g3		10	462.19	61.918	346.18	308.44			0.99996
	g4		10	577.49	59.922	427.47	294.72			0.99996
	g5		10	559.10	59.603	365.61	279.44			0.99996
				temperature range of fits 5 to 300eV						
Ar^{2+}	g1	6	10	1157.1	47.150	723.90	206.63			0.99993
	g2		10	1205.0	47.067	781.52	207.39			0.99992
	g3		10	1209.9	46.972	776.30	207.37			0.99993
	g4		10	1421.1	44.561	785.40	201.32			0.99993
	g5		10	2071.8	41.649	1159.50	196.33			0.99989

TABLE III. Radiative Cooling Rate for Argon Ions
See page 236 for Explanation of Tables

ArII

n_e (cm^{-3})	T_e (eV) 2	4	6	8	10	12
1[+03]	8.38[−19]	6.67[−17]	3.05[−16]	6.56[−16]	1.04[−15]	1.40[−15]
1[+06]	8.49[−16]	6.73[−14]	3.07[−13]	6.54[−13]	1.04[−12]	1.40[−12]
1[+08]	8.59[−14]	6.82[−12]	3.10[−11]	6.65[−11]	1.05[−10]	1.41[−10]
1[+10]	8.59[−12]	6.83[−10]	3.05[−09]	6.65[−09]	1.05[−08]	1.41[−08]
1[+12]	8.66[−10]	6.91[−08]	3.14[−07]	6.59[−07]	1.06[−06]	1.41[−06]
1[+14]	9.05[−08]	7.63[−06]	3.42[−05]	7.17[−05]	1.11[−04]	1.46[−04]

ArIII

	2	5	8	11	14	16
1[+03]	1.04[−17]	1.01[−16]	4.55[−16]	9.90[−16]	1.55[−15]	1.91[−15]
1[+06]	8.43[−15]	9.87[−14]	4.54[−13]	9.88[−13]	1.55[−12]	1.91[−12]
1[+08]	5.23[−13]	9.89[−12]	4.62[−11]	9.98[−11]	1.55[−10]	1.91[−10]
1[+10]	8.97[−12]	8.73[−10]	4.53[−09]	9.93[−09]	1.55[−08]	1.90[−08]
1[+12]	7.04[−10]	8.67[−08]	4.52[−07]	9.94[−07]	1.55[−06]	1.90[−06]
1[+14]	6.69[−08]	9.10[−06]	4.73[−05]	1.01[−04]	1.55[−04]	1.87[−04]

ArIV

	3	7	10	14	18	21
1[+03]	2.06[−17]	2.32[−16]	6.18[−16]	1.24[−15]	1.82[−15]	2.20[−15]
1[+06]	2.10[−14]	2.37[−13]	6.29[−13]	1.25[−12]	1.84[−12]	2.23[−12]
1[+08]	1.63[−12]	2.39[−11]	6.35[−11]	1.27[−10]	1.85[−10]	2.24[−10]
1[+10]	6.31[−11]	2.30[−09]	6.42[−09]	1.29[−08]	1.89[−08]	2.27[−08]
1[+12]	5.19[−09]	2.29[−07]	6.44[−07]	1.29[−06]	1.89[−06]	2.27[−06]
1[+14]	5.11[−07]	2.31[−05]	6.46[−05]	1.28[−04]	1.85[−04]	2.21[−04]

ArV

	7	9	11	15	18	22
1[+03]	2.67[−16]	5.18[−16]	8.02[−16]	1.37[−15]	1.75[−15]	2.17[−15]
1[+06]	2.61[−13]	5.17[−13]	8.01[−13]	1.36[−12]	1.74[−12]	2.17[−12]
1[+08]	2.67[−11]	5.22[−11]	8.08[−11]	1.38[−10]	1.76[−10]	2.18[−10]
1[+10]	2.61[−09]	5.17[−09]	8.06[−09]	1.38[−08]	1.76[−08]	2.19[−08]
1[+12]	2.60[−07]	5.15[−07]	8.05[−07]	1.38[−06]	1.76[−06]	2.19[−06]
1[+14]	2.55[−05]	5.08[−05]	7.93[−05]	1.35[−04]	1.73[−04]	2.14[−04]

ArVI

	9	10	18	27	36	45
1[+03]	5.84[−16]	7.24[−16]	1.77[−15]	2.53[−15]	3.04[−15]	3.68[−15]
1[+06]	5.85[−13]	7.26[−13]	1.78[−12]	2.54[−12]	3.05[−12]	3.68[−12]
1[+08]	5.91[−11]	7.33[−11]	1.79[−10]	2.54[−10]	3.05[−10]	3.68[−10]
1[+10]	5.91[−09]	7.33[−09]	1.79[−08]	2.54[−08]	3.04[−08]	3.67[−08]
1[+12]	5.90[−07]	7.31[−07]	1.78[−06]	2.53[−06]	3.03[−06]	3.65[−06]
1[+14]	5.55[−05]	6.86[−05]	1.65[−04]	2.33[−04]	2.76[−04]	3.26[−04]

TABLE III. Radiative Cooling Rate for Argon Ions

See page 236 for Explanation of Tables

ArVII

n_e (cm^{-3})	T_e (eV) 12	24	37	49	62	74
1[+03]	1.21[−15]	2.36[−15]	2.87[−15]	3.08[−15]	3.20[−15]	3.26[−15]
1[+06]	1.21[−12]	2.35[−12]	2.86[−12]	3.07[−12]	3.19[−12]	3.25[−12]
1[+08]	1.15[−10]	2.20[−10]	2.66[−10]	2.86[−10]	2.98[−10]	3.04[−10]
1[+10]	1.13[−08]	2.16[−08]	2.62[−08]	2.81[−08]	2.93[−08]	2.99[−08]
1[+12]	1.13[−06]	2.15[−06]	2.61[−06]	2.80[−06]	2.91[−06]	2.97[−06]
1[+14]	9.49[−05]	1.74[−04]	2.08[−04]	2.23[−04]	2.29[−04]	2.37[−04]

ArVIII

	14	28	42	57	71	85
1[+03]	8.85[−16]	1.32[−15]	1.46[−15]	1.53[−15]	1.56[−15]	1.60[−15]
1[+06]	8.85[−13]	1.32[−12]	1.46[−12]	1.53[−12]	1.56[−12]	1.60[−12]
1[+08]	8.85[−11]	1.32[−10]	1.46[−10]	1.53[−10]	1.56[−10]	1.60[−10]
1[+10]	8.85[−09]	1.32[−08]	1.46[−08]	1.53[−08]	1.56[−08]	1.60[−08]
1[+12]	8.85[−07]	1.32[−06]	1.46[−06]	1.53[−06]	1.56[−06]	1.60[−06]
1[+14]	8.82[−05]	1.32[−04]	1.46[−04]	1.52[−04]	1.56[−04]	1.60[−04]

ArIX

	42	63	84	110	130	210
1[+03]	3.41[−18]	3.04[−17]	9.02[−17]	1.93[−16]	2.80[−16]	5.93[−16]
1[+06]	3.41[−15]	3.04[−14]	9.02[−14]	1.93[−13]	2.80[−13]	5.93[−13]
1[+08]	3.41[−13]	3.04[−12]	9.02[−12]	1.93[−11]	2.80[−11]	5.93[−11]
1[+10]	3.43[−11]	3.05[−10]	9.05[−10]	1.94[−09]	2.81[−09]	5.94[−09]
1[+12]	3.58[−09]	3.18[−08]	9.40[−08]	2.00[−07]	2.89[−07]	6.04[−07]
1[+14]	3.63[−07]	3.22[−06]	9.52[−06]	2.03[−05]	2.92[−05]	6.08[−05]

ArX

	47	95	140	190	240	290
1[+03]	4.64[−17]	1.80[−16]	3.47[−16]	5.56[−16]	7.16[−16]	7.38[−16]
1[+06]	4.64[−14]	1.80[−13]	3.47[−13]	5.56[−13]	7.16[−13]	7.38[−13]
1[+08]	4.64[−12]	1.80[−11]	3.47[−11]	5.56[−11]	7.16[−11]	7.39[−11]
1[+10]	4.62[−10]	1.79[−09]	3.47[−09]	5.56[−09]	7.15[−09]	7.38[−09]
1[+12]	4.55[−08]	1.79[−07]	3.46[−07]	5.55[−07]	7.14[−07]	7.37[−07]
1[+14]	4.55[−06]	1.78[−05]	3.46[−05]	5.55[−05]	7.14[−05]	7.37[−05]

ArXI

	53	110	160	220	270	320
1[+03]	1.11[−16]	2.45[−16]	3.95[−16]	5.60[−16]	6.91[−16]	7.82[−16]
1[+06]	1.11[−13]	2.45[−13]	3.95[−13]	5.60[−13]	6.91[−13]	7.82[−13]
1[+08]	1.11[−11]	2.45[−11]	3.95[−11]	5.60[−11]	6.91[−11]	7.81[−11]
1[+10]	1.11[−09]	2.45[−09]	3.96[−09]	5.61[−09]	6.92[−09]	7.82[−09]
1[+12]	1.07[−07]	2.45[−07]	3.98[−07]	5.63[−07]	6.95[−07]	7.86[−07]
1[+14]	1.03[−05]	2.44[−05]	3.98[−05]	5.64[−05]	6.97[−05]	7.88[−05]

TABLE III. Radiative Cooling Rate for Argon Ions

See page 236 for Explanation of Tables

ArXII

n_e (cm^{-3})	T_e (eV) 61	120	190	250	310	370
1[+03]	1.91[−16]	2.99[−16]	4.53[−16]	5.71[−16]	6.64[−16]	7.36[−16]
1[+06]	1.91[−13]	2.99[−13]	4.53[−13]	5.71[−13]	6.64[−13]	7.36[−13]
1[+08]	1.91[−11]	2.99[−11]	4.53[−11]	5.71[−11]	6.64[−11]	7.37[−11]
1[+10]	1.87[−09]	2.99[−09]	4.55[−09]	5.73[−09]	6.66[−09]	7.38[−09]
1[+12]	1.78[−07]	2.99[−07]	4.58[−07]	5.77[−07]	6.71[−07]	7.43[−07]
1[+14]	1.74[−05]	3.01[−05]	4.63[−05]	5.83[−05]	6.77[−05]	7.49[−05]

ArXIII

	68	140	210	270	340	410
1[+03]	2.46[−16]	3.62[−16]	4.78[−16]	5.63[−16]	6.41[−16]	7.01[−16]
1[+06]	2.46[−13]	3.62[−13]	4.78[−13]	5.63[−13]	6.41[−13]	7.01[−13]
1[+08]	2.45[−11]	3.63[−11]	4.78[−11]	5.63[−11]	6.42[−11]	7.01[−11]
1[+10]	2.46[−09]	3.63[−09]	4.79[−09]	5.65[−09]	6.43[−09]	7.02[−09]
1[+12]	2.47[−07]	3.67[−07]	4.83[−07]	5.68[−07]	6.46[−07]	7.06[−07]
1[+14]	2.45[−05]	3.68[−05]	4.84[−05]	5.70[−05]	6.48[−05]	7.07[−05]

ArXIV

	160	230	300	380	450	760
1[+03]	3.46[−16]	4.13[−16]	4.70[−16]	5.21[−16]	5.53[−16]	6.30[−16]
1[+06]	3.46[−13]	4.13[−13]	4.70[−13]	5.20[−13]	5.53[−13]	6.30[−13]
1[+08]	3.46[−11]	4.13[−11]	4.69[−11]	5.21[−11]	5.53[−11]	6.30[−11]
1[+10]	3.45[−09]	4.13[−09]	4.69[−09]	5.20[−09]	5.52[−09]	6.29[−09]
1[+12]	3.44[−07]	4.11[−07]	4.67[−07]	5.18[−07]	5.51[−07]	6.28[−07]
1[+14]	3.42[−05]	4.10[−05]	4.66[−05]	5.17[−05]	5.50[−05]	6.26[−05]

ArXV

	170	260	340	430	510	860
1[+03]	3.28[−16]	3.71[−16]	4.03[−16]	4.29[−16]	4.46[−16]	4.79[−16]
1[+06]	3.28[−13]	3.71[−13]	4.03[−13]	4.29[−13]	4.46[−13]	4.79[−13]
1[+08]	3.28[−11]	3.71[−11]	4.03[−11]	4.29[−11]	4.46[−11]	4.79[−11]
1[+10]	3.26[−09]	3.69[−09]	4.02[−09]	4.28[−09]	4.44[−09]	4.78[−09]
1[+12]	3.13[−07]	3.58[−07]	3.91[−07]	4.19[−07]	4.37[−07]	4.74[−07]
1[+14]	3.10[−05]	3.56[−05]	3.90[−05]	4.18[−05]	4.36[−05]	4.72[−05]

ArXVI

	180	370	550	730	920	1100
1[+03]	1.72[−16]	2.05[−16]	2.27[−16]	2.40[−16]	1.25[−18]	2.54[−16]
1[+06]	1.72[−13]	2.05[−13]	2.27[−13]	2.40[−13]	1.25[−15]	2.54[−13]
1[+08]	1.72[−11]	2.05[−11]	2.27[−11]	2.40[−11]	1.25[−13]	2.54[−11]
1[+10]	1.72[−09]	2.05[−09]	2.27[−09]	2.40[−09]	1.25[−11]	2.54[−09]
1[+12]	1.72[−07]	2.05[−07]	2.27[−07]	2.40[−07]	1.25[−09]	2.54[−07]
1[+14]	1.72[−05]	2.05[−05]	2.27[−05]	2.40[−05]	1.25[−07]	2.54[−05]

TABLE III. Radiative Cooling Rate for Argon Ions

See page 236 for Explanation of Tables

ArXVII

n_e (cm^{-3})	T_e (eV) 820	1700	2500	3300	4100	5000
1[+03]	4.52[−18]	2.69[−17]	4.43[−17]	5.67[−17]	6.56[−17]	7.30[−17]
1[+06]	4.52[−15]	2.69[−14]	4.43[−14]	5.67[−14]	6.56[−14]	7.30[−14]
1[+08]	4.52[−13]	2.69[−12]	4.43[−12]	5.67[−12]	6.56[−12]	7.29[−12]
1[+10]	4.52[−11]	2.69[−10]	4.43[−10]	5.67[−10]	6.56[−10]	7.30[−10]
1[+12]	4.52[−09]	2.69[−08]	4.44[−08]	5.68[−08]	6.57[−08]	7.30[−08]
1[+14]	4.53[−07]	2.69[−06]	4.44[−06]	5.68[−06]	6.57[−06]	7.31[−06]

ArXVIII

	900	1800	2700	3500	4400	5300
1[+03]	2.63[−18]	2.52[−18]	2.34[−17]	2.93[−17]	3.42[−17]	3.76[−17]
1[+06]	2.63[−15]	2.52[−15]	2.34[−14]	2.93[−14]	3.42[−14]	3.76[−14]
1[+08]	2.63[−13]	2.52[−13]	2.34[−12]	2.93[−12]	3.42[−12]	3.76[−12]
1[+10]	2.63[−11]	2.52[−11]	2.34[−10]	2.93[−10]	3.42[−10]	3.76[−10]
1[+12]	2.63[−09]	2.52[−09]	2.34[−08]	2.93[−08]	3.42[−08]	3.76[−08]
1[+14]	2.63[−07]	2.52[−07]	2.33[−06]	2.93[−06]	3.42[−06]	3.76[−06]

TABLE IV. Fitting Coefficients for Argon Cooling Coefficient

See page 236 for Explanation of Tables

T_e (keV)	M_0	M_1	M_2
0.002 − 0.02	−3.7573[−20]	2.8398[−17]	−7.4088[−15]
0.02 − 0.065	−3.7246[−17]	4.8144[−15]	−2.1810[−13]
0.065 − 0.2	−6.7663[−20]	1.6671[−17]	−4.0182[−16]
0.2 − 0.5	1.4904[−18]	−3.4108[−17]	3.2167[−16]
0.5 − 0.9	2.2089[−18]	−1.1151[−17]	2.2525[−17]
0.9 − 5.0	4.2162[−20]	−3.5203[−21]	7.1270[−21]
5.0 − 19.0	5.3129[−20]	−1.5258[−20]	2.1341[−21]
T_e	M_3	M_4	M_5
0.002 − 0.02	2.2873[−12]	-1.3614[−10]	2.4647[−09]
0.02 − 0.065	4.5963[−12]	-4.6126[−11]	1.7843[−10]
0.065 − 0.2	4.1981[−15]	-1.8615[−14]	2.9787[−14]
0.2 − 0.5	−1.2500[−15]	2.1331[−15]	−1.3383[−15]
0.5 − 0.9	−2.1518[−17]	9.0461[−18]	−1.0548[−18]
0.9 − 5.0	−5.6864[−21]	1.3587[−21]	−1.0469[−22]
5.0 − 19.0	−1.5156[−22]	5.3549[−24]	−7.4667[−26]

See page 237 for Explanation of Graphs

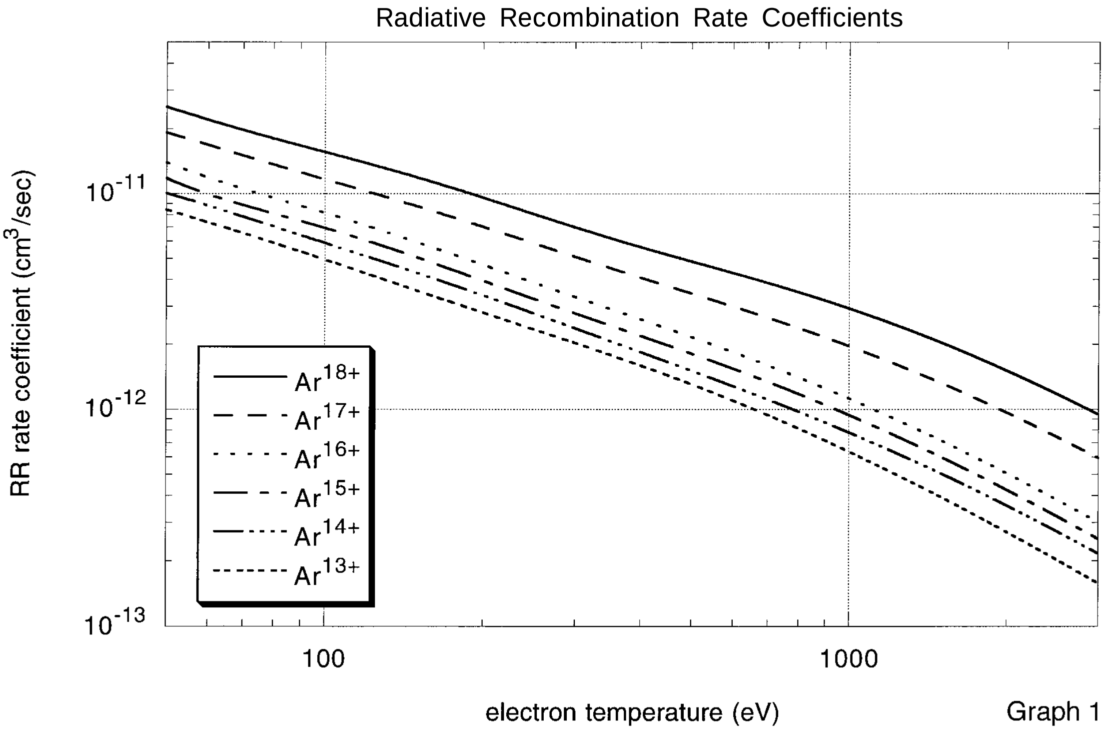

Graph 1

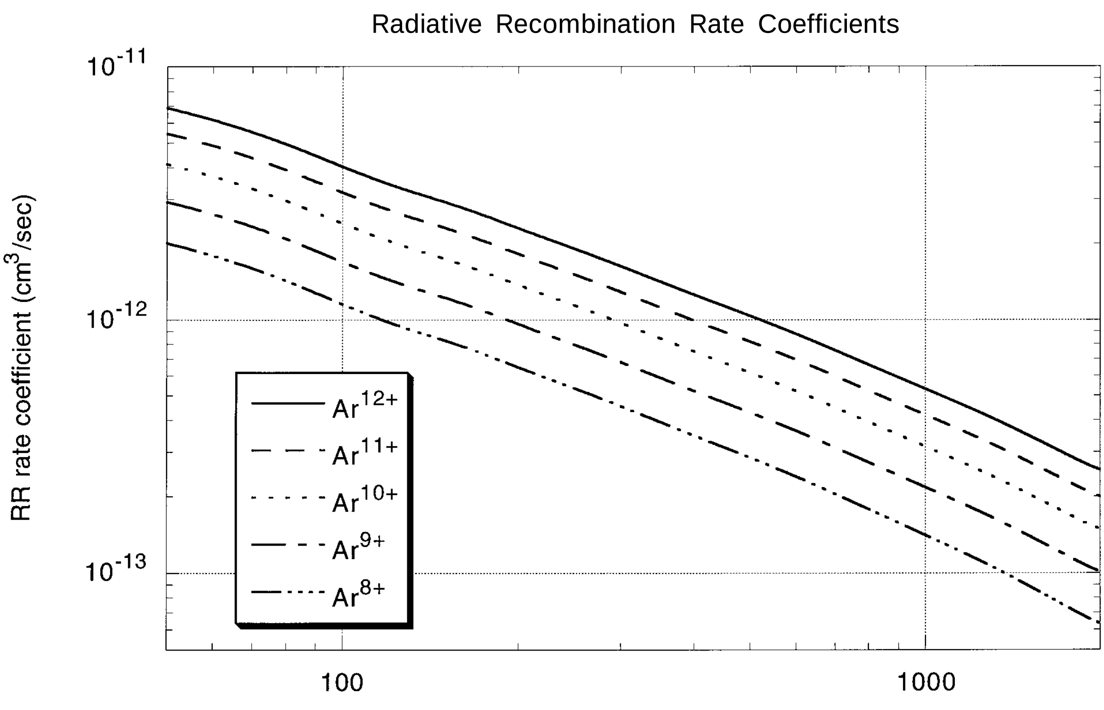

Graph 2

See page 237 for Explanation of Graphs

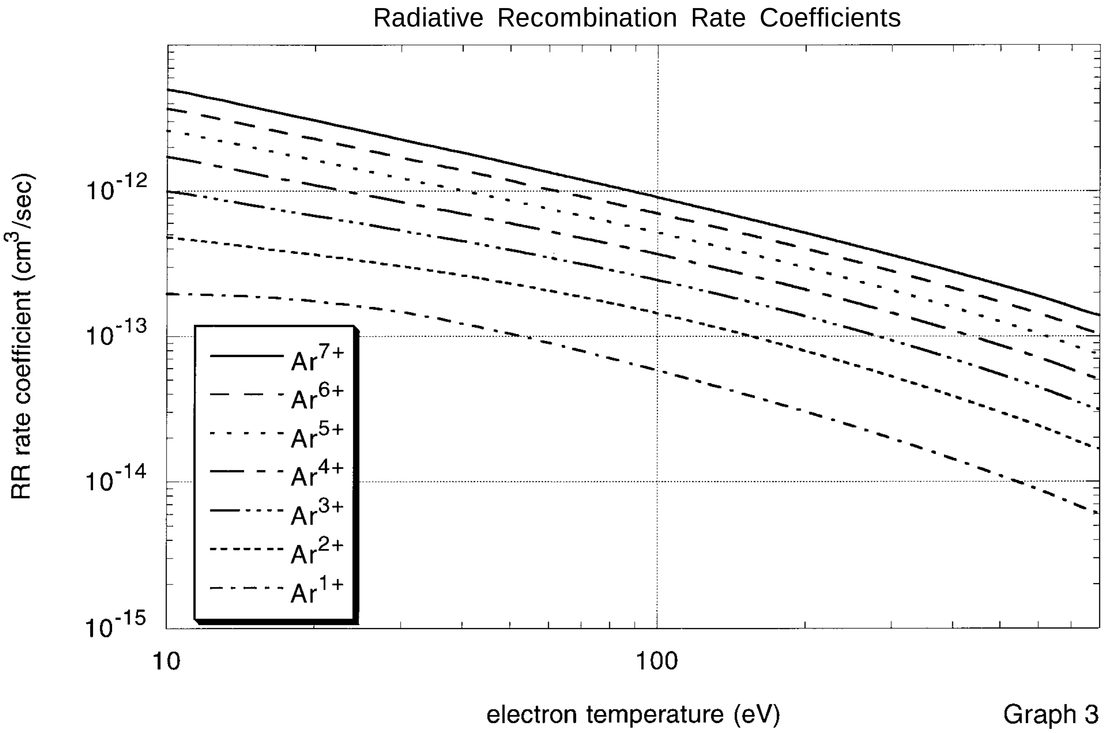

Graph 3

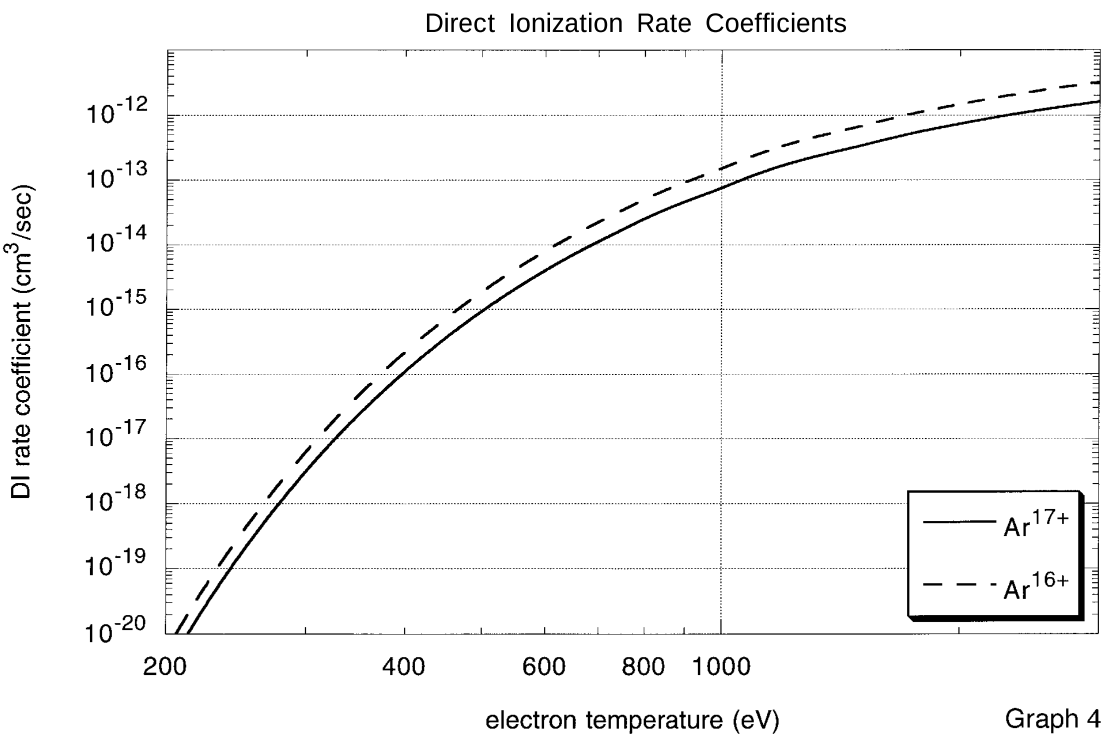

Graph 4

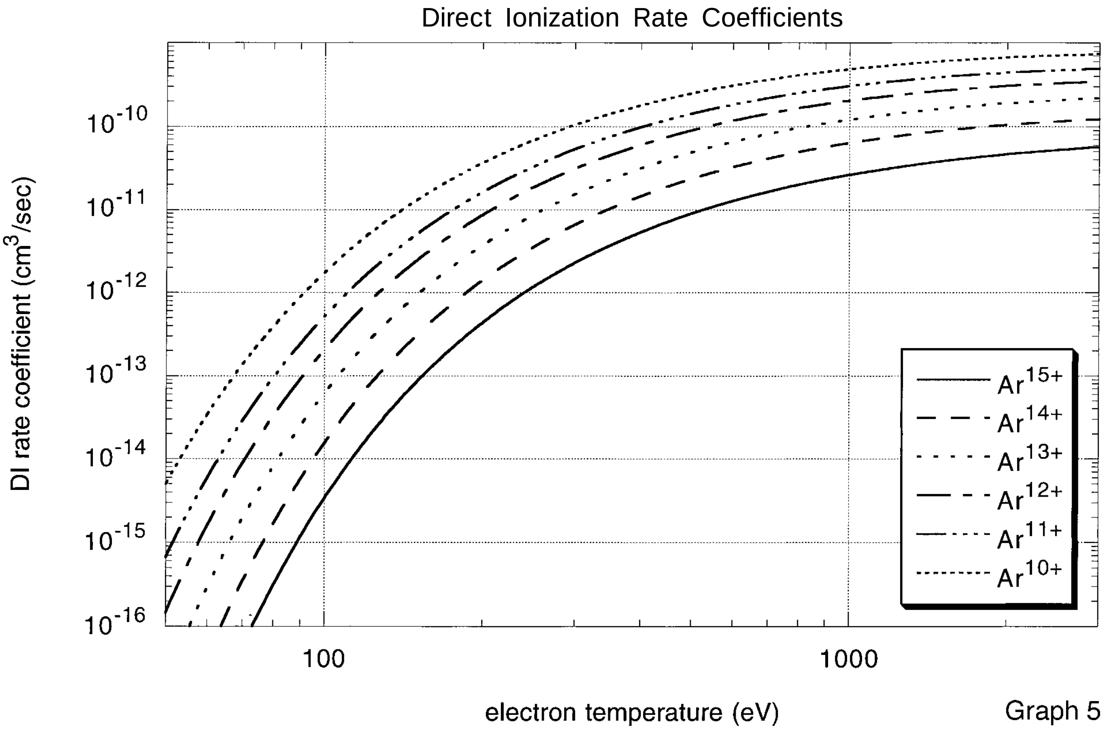

Graph 5

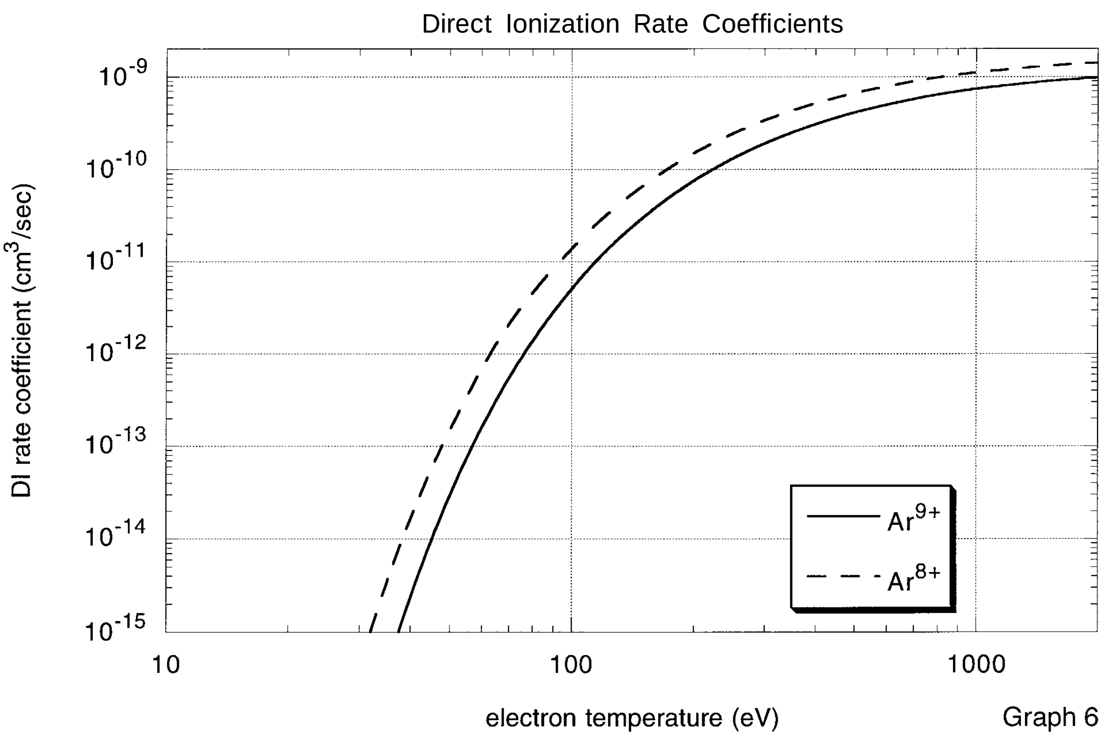

Graph 6

See page 237 for Explanation of Graphs

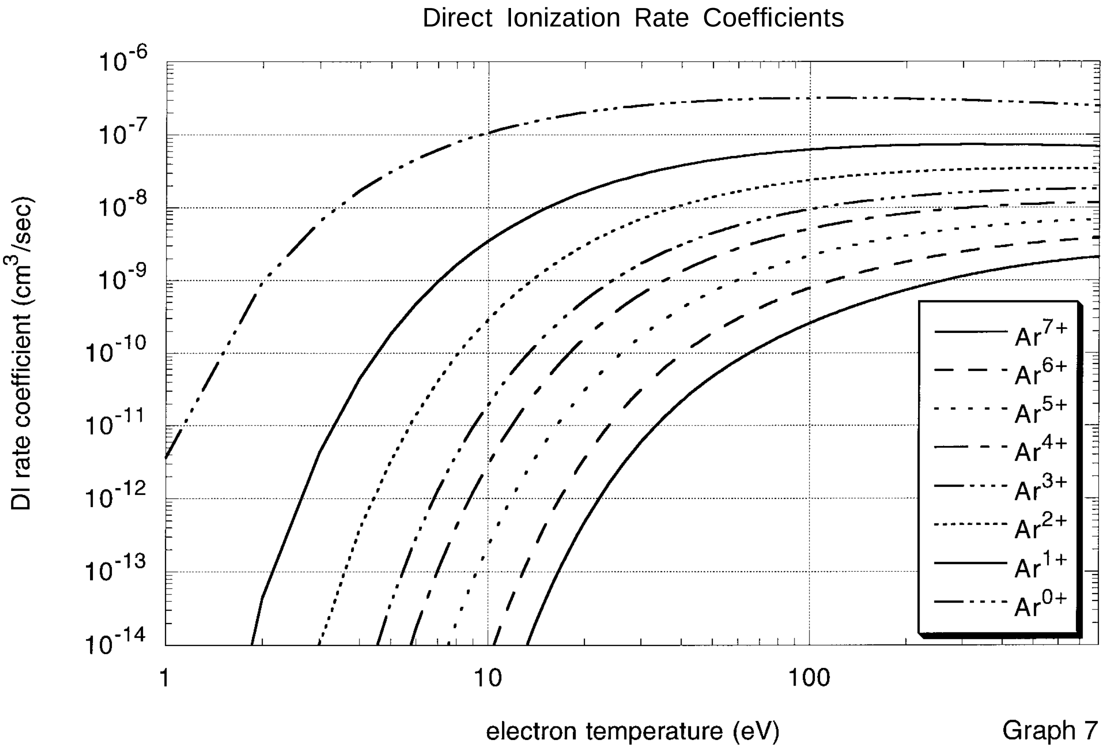

Graph 7

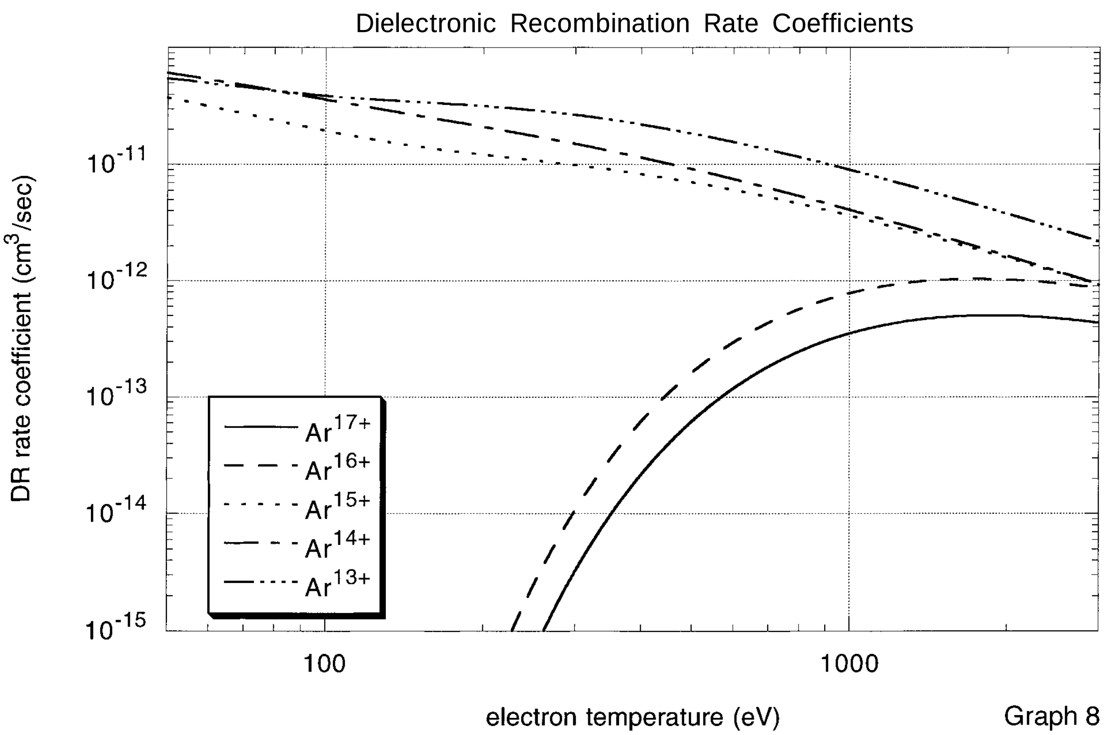

Graph 8

See page 237 for Explanation of Graphs

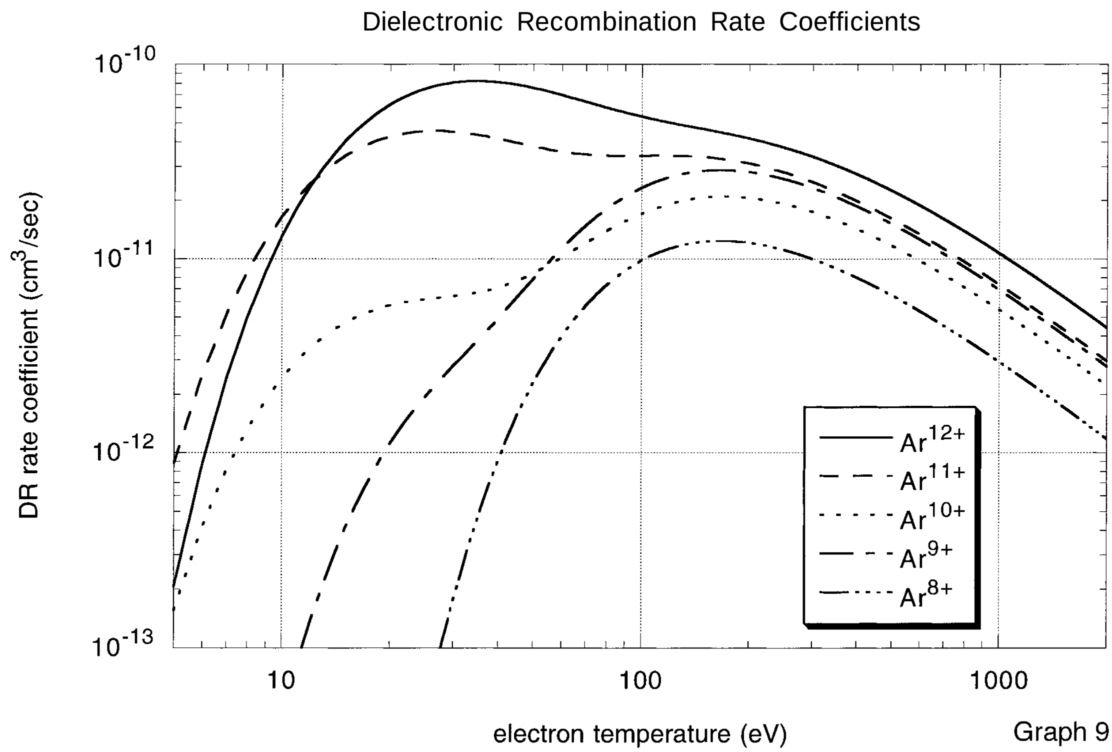

Graph 9

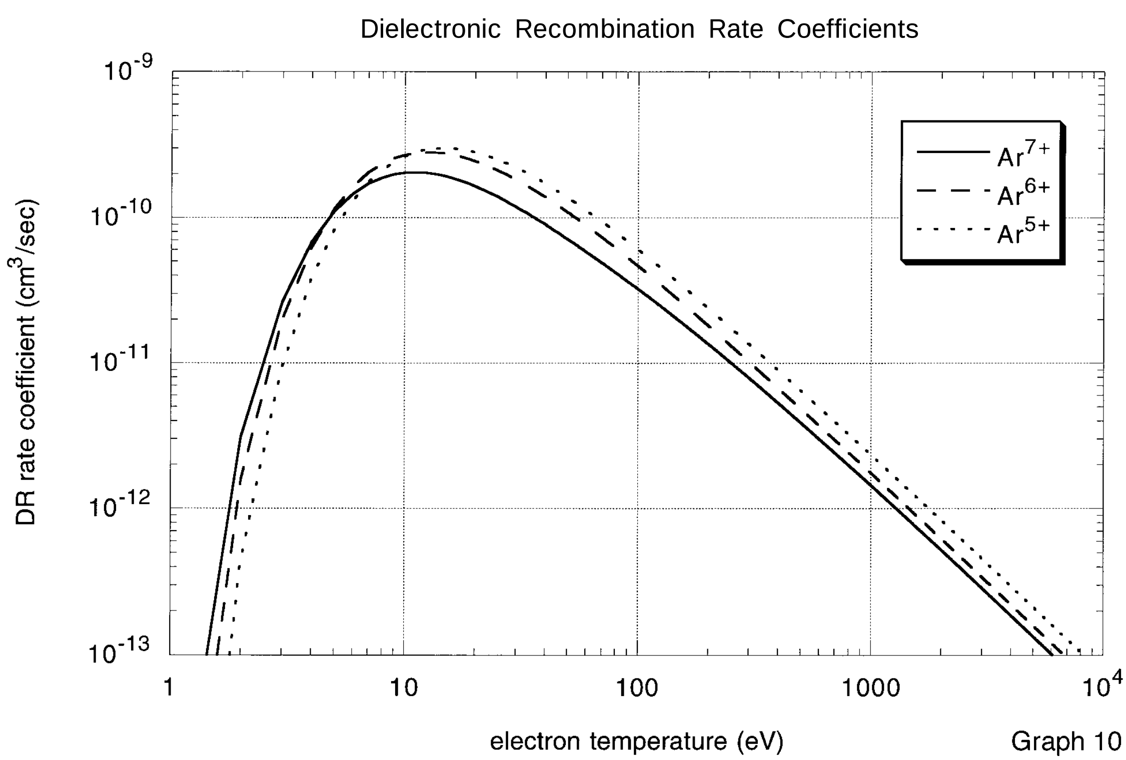

Graph 10

See page 237 for Explanation of Graphs

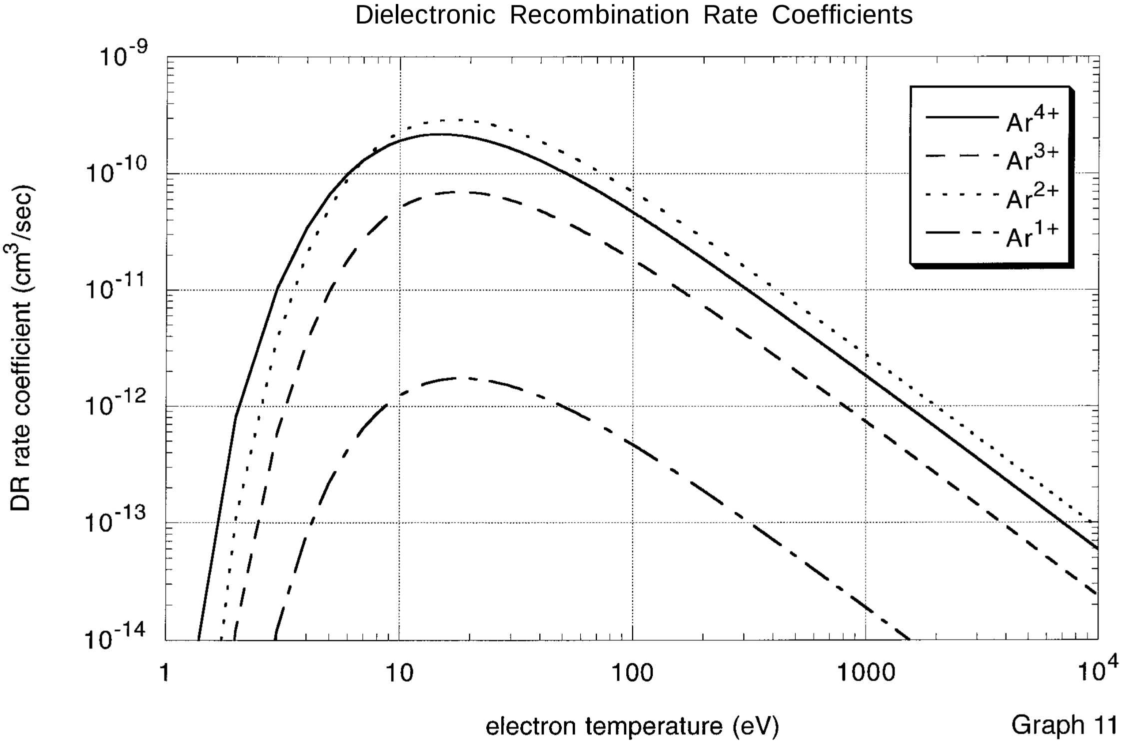

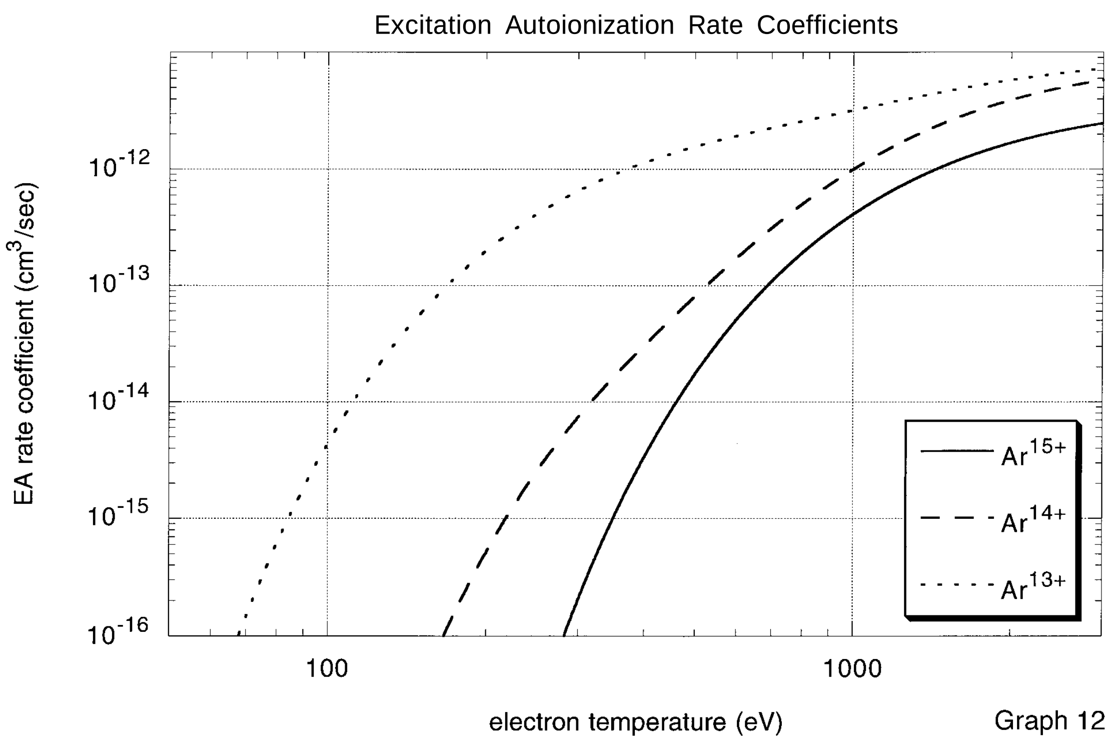

See page 237 for Explanation of Graphs

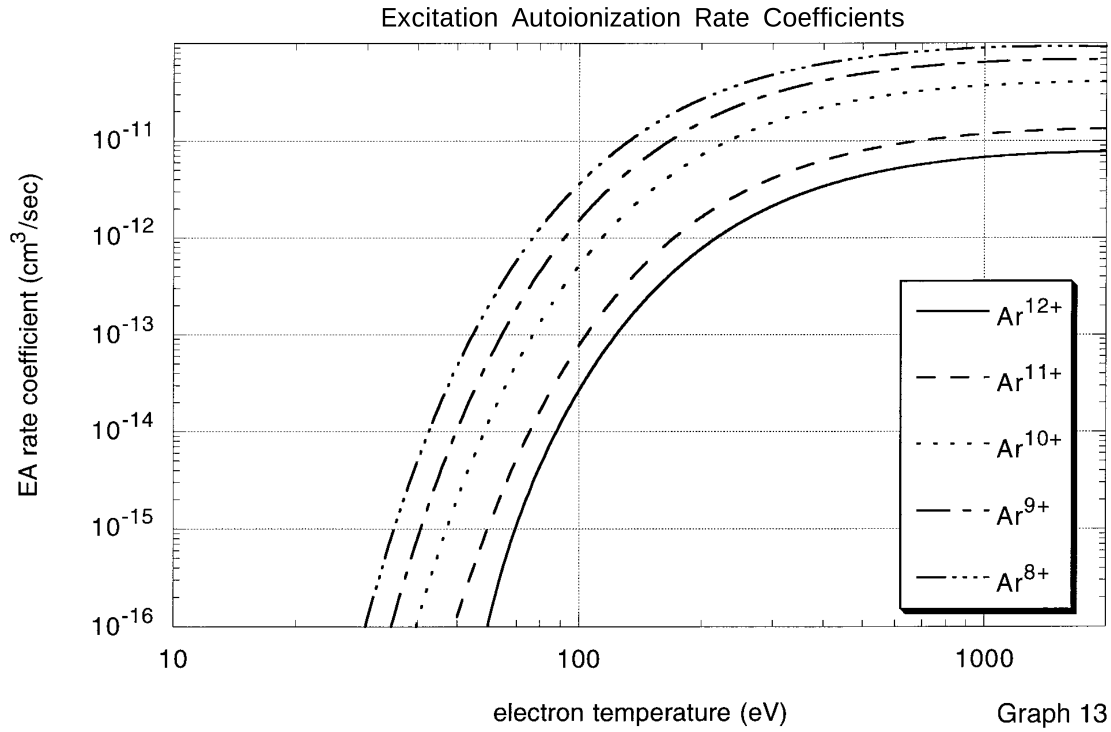

Graph 13

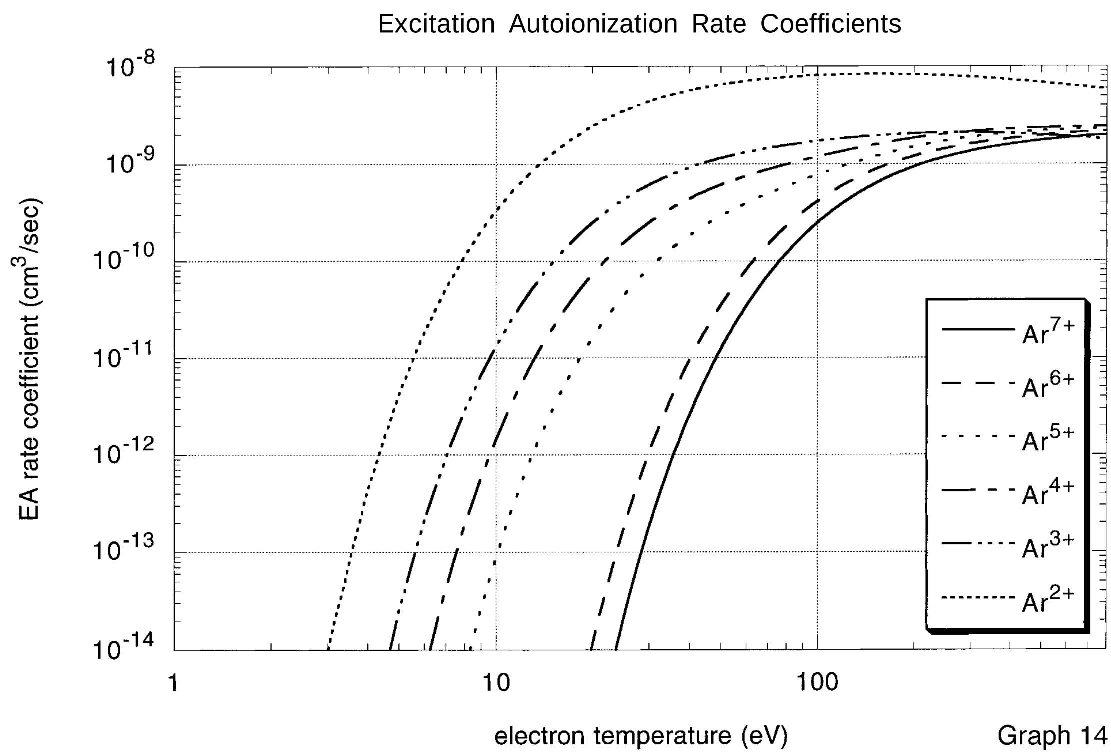

Graph 14